Sultan, Md Tipu; Altgen, Daniela; Awais, Muhammad; Rautkari, Lauri; Altgen, Michael

Impact of a conditioning step during the treatment of wood with melamine-formaldehyde resin on dimensional stabilisation

Published in:
Holzforschung

DOI:
10.1515/hf-2023-0084

Published: 01/01/2024

Document Version
Publisher's PDF, also known as Version of record

Published under the following license:
Unspecified

Please cite the original version:
Sultan, M. T., Altgen, D., Awais, M., Rautkari, L., & Altgen, M. (2024). Impact of a conditioning step during the treatment of wood with melamine-formaldehyde resin on dimensional stabilisation. *Holzforschung*, *78*(1), 37-46. https://doi.org/10.1515/hf-2023-0084

Wood Technology/Products

Md. Tipu Sultan, Daniela Altgen, Muhammad Awais, Lauri Rautkari and Michael Altgen*

Impact of a conditioning step during the treatment of wood with melamine-formaldehyde resin on dimensional stabilisation

https://doi.org/10.1515/hf-2023-0084
Received August 14, 2023; accepted October 24, 2023;
published online November 24, 2023

Abstract: The dimensional stabilisation of wood using thermosetting resins relies on the resin uptake into the cell walls. This study tested if a conditioning step after the impregnation and before the final heat-curing enhances the cell wall uptake to improve dimensional stabilisation without increasing the chemical consumption. Small blocks of Scots pine sapwood were vacuum-impregnated with an aqueous melamine formaldehyde solution and conditioned at 33, 70, or 95 % RH for up to 1 week before drying and curing the blocks at 103 °C. However, the conditioning step decreased the cell wall bulking and the moisture exclusion effect compared to the immediate heat curing of the impregnated samples. Analyses of the resin-treated samples by scanning electron microscopy, IR spectroscopy and confocal Raman microspectroscopy provided evidence of wood hydrolysis and polycondensation of the resin within the cell lumen during the conditioning step. Hydrolysis and removal of wood constituents may have counterbalanced the cell wall bulking of the resin. Polycondensation of the resin in the lumen increased its molecule size, which could have hindered the cell wall diffusion of the resin.

Keywords: thermosetting resin; vibrational spectroscopy; water vapour sorption; wood modification

***Corresponding author: Michael Altgen**, Department of Wood Technology, Norwegian Institute of Bioeconomy Research, P.O. Box 115, 1431 Ås, Norway, E-mail: michael.altgen@nibio.no. https://orcid.org/0000-0002-0024-8677
Md. Tipu Sultan, Muhammad Awais and Lauri Rautkari, Department of Bioproducts and Biosystems, School of Chemical Engineering, Aalto University, P.O. Box 16300, 00076 Aalto, Finland
Daniela Altgen, Norwegian Institute of Wood Technology, P.O. Box 113 Blindern, 0314 Oslo, Norway

1 Introduction

The dimensional stabilisation of wood by thermosetting resins and other modification agents to extend the wood's service life relies on the chemical uptake into the wood cell walls and cannot be achieved by lumen filling (Furuno et al. 2004; Ohmae et al. 2002). The fixation of the modification agents within the cell wall causes permanent cell wall bulking that limits the cell wall space available for water and improves the resistance against fungal decay (Biziks et al. 2020; Thybring 2013). The uptake of modification agents by the cell wall is mainly dependent on their molecular size (Biziks et al. 2020; Furuno et al. 2004), their concentration within the solution (Altgen et al. 2020b; Hu et al. 2022), and the nature of the solvent (Jeremic et al. 2007; Thygesen et al. 2020). However, the conditions during the impregnation, drying and heat-curing steps of the modification treatment also affect the cell wall bulking (Altgen et al. 2023; Klüppel and Mai 2013). Therefore, careful selection of treatment conditions may improve the cell wall bulking without increasing the chemical consumption during the modification.

During the impregnation step of the modification, the aqueous solution containing the modification agent flows through the coarse wood structure driven by the applied vacuum and/or pressure. The water (solvent) causes the cell walls to swell, which creates space in the cell wall for the modification agent to enter if the molecules are small enough. The concentration of modification agent in the swollen structure (i.e. cell wall) and the free water (i.e. cell lumen) may be assumed to be uniform in the fully impregnated wood (Klüppel and Mai 2013; Stamm 1934). Removing free water from the lumen during the subsequent drying increases the concentration of the modification agent in the cell lumen, and thus promotes solute diffusion into the cell walls (Klüppel and Mai 2013; Stamm 1956). However, removing bound water from the cell wall reduces the free volume and molecular motions in the polymer matrix, hindering cell wall diffusion (Jakes et al. 2019).

Since diffusion is time-dependent, one may assume a conditioning phase under suitable atmospheric conditions to

improve the cell wall uptake in the impregnated wood. However, the mechanism of solute diffusion becomes more complex when using melamine-formaldehyde (MF) resin or other thermosetting resins as modification agents and contrasting results have been reported. Zheng et al. (2018) found a conditioning phase at elevated relative humidity to improve the solute diffusion of MF resin into wood cell walls. In contrast, Klüppel and Mai (2013) reported that conditioning phenol-formaldehyde resin-impregnated samples for 1 week in a desiccator over water reduced the cell wall bulking effect compared to the immediate drying and heat-curing. This may be explained by the polycondensation of the resin during the conditioning step, which may form macromolecules in the cell lumen of impregnated wood that are too large to enter the cell wall (Klüppel and Mai 2013). Furthermore, the alkaline pH of the resin solution in combination with the elevated temperatures during the drying and curing of the impregnated wood could cause some hydrolysis of cell wall constituents (Altgen et al. 2020b).

In the present study, Scots pine sapwood was treated with low molecular weight MF resin and the effect of conditioning resin-impregnated samples at different relative humidity (RH) levels (33, 70, and 95 % RH) and durations (0, 72 and 168 h) on the cell wall bulking and water vapour sorption was tested. It was hypothesized that the dimensional stabilisation of resin-treated wood is affected by two mechanisms that take place during the conditioning phase: (a) alkaline hydrolysis removes cell wall polymers and counterbalances the cell wall bulking effect of the resin; and/or (b) self-condensation of the resin within the lumen increases the molecule size during the conditioning, which hinders its cell wall diffusion.

2 Materials and methods

2.1 Materials

Samples with dimensions of ca. 20 × 20 × 10 mm (radial × tangential × longitudinal) were prepared from commercially kiln-dried boards of Scots pine (*Pinus sylvestris* L.) originating from Southeast Finland. Knots, visible defects, juvenile wood, and heartwood were avoided. All samples were cut from the same annual rings to limit raw material-based variation, especially in bulk density.

Low molecular weight melamine formaldehyde (MF, Madurit MW 840, Prefere Resins, Finland) was obtained as a stock solution with a solid resin content of ca. 68 %, which was determined as the non-volatile dry matter remaining after drying at 103 °C. The received MF resin was partially methylated to limit self-condensation during storage and improve miscibility with water. The stock solution was stored at 6 °C for several weeks before the experiments.

Polyethylene glycol (PEG; CAS 25322-68-3) with an average molecular mass of 1900–2200 (PEG-2000) was obtained from Sigma-Aldrich.

2.2 Impregnation treatments

The wood samples were treated with MF resin or PEG. PEG-treated wood samples served as references to resin-treated samples because an aqueous PEG solution is unlikely to cause wood hydrolysis during the treatment and the molecular size of PEG does not change through self-condensation.

Aqueous solutions with 20 % solid content were prepared from the PEG and the MF stock solution. The wood samples were impregnated with either the PEG or the MF solution at 0.004 MPa for 1 h. After removing the samples from the solution, excess solution at the wood surface was removed and the different sample groups (n = 10) were conditioned at 20 °C in desiccators at three relative humidity levels (33, 70, and 95 % RH) and two durations (72 and 168 h). Different RH levels were achieved by the addition of aqueous, supersaturated salt solutions of either magnesium chloride, potassium iodide, or potassium nitrate to the desiccators (Greenspan 1977). One sample group per impregnation solution was immediately heat-cured without any intermediate conditioning step. Drying and heat-curing were performed in a convection oven in two temperature steps at 40 and 103 °C, with each temperature held for ca. 24 h.

2.3 Changes in sample mass and dimensions

Mass and dimensions were recorded for all samples in the oven-dry state (103 °C for ca. 24 h) before and after the impregnation treatment. Changes in dry mass and dimensions were calculated as weight percent gain (WPG) and cell wall bulking (CWB), respectively, as described previously (Klüppel and Mai 2013). Only the cross-sectional area was considered because the changes in longitudinal direction were negligible. WPG and CWB of the resin-treated samples were determined again after a water-leaching protocol. This involved vacuum-impregnating the samples with deionized water for 1 h at 0.004 MPa and storage of the submerged samples with ca. five volumes of water per one volume of wood for 1 week with daily water changes. The water-leached samples were re-dried at 20, 60, and finally 103 °C for 24 h, respectively. All analyses were performed on water-leached samples.

2.4 Dynamic vapour sorption

Sorption isotherms of wood samples were measured with an automated sorption balance (DVS intrinsic, Surface Measurement Systems, UK). In addition to an untreated reference sample, resin-treated samples that were either not conditioned before curing or conditioned for 168 h were measured. For the measurement, a thin section containing early- and latewood weighing approximately 15 mg was cut from the centre of the corresponding wood sample using a razor blade. Absorption isotherms were measured using a RH sequence of 0, 5, 15, 25, 35, 45, 55, 65, 75, 85, and 95 %. Desorption isotherms were measured using the same RH sequence in the reverse order. The temperature and the nitrogen flow rate were maintained at 25 °C and 200 sccm, respectively. Each RH step was maintained until the rate of sample mass change over time remained below 0.0005 % min^{-1} for 10 min. This rate was determined in a ten-minute regression window. The moisture content (MC) was calculated by relating the mass of absorbed water to the dry sample mass. From the MCs at the end of each RH step, the MC ratio was calculated by relating the MC of a treated sample to the MC of the untreated reference sample at each RH step.

2.5 Scanning electron microscopy

For scanning electron microscopy (SEM), small cubes with approx. 5 mm edge lengths were cut from the centre of each sample using a razor blade. The cubes were soaked in deionized water and one radial surface was smoothened with a sledge microtome (WSL Lab-Microtome, Swiss Federal Research Institute WSL, Switzerland). The smoothened cubes were dried and coated with gold–palladium before analysis was performed with a scanning electron microscope (Zeiss, Sigma VP, Germany). Images were taken using a beam acceleration voltage of 2 kV and a detector for secondary electrons.

2.6 Infrared spectroscopy

Selected samples were split in half and thin sections were cut from the longitudinal-radial surface using a razor blade. The sections were stored at ambient laboratory conditions before the measurements. Mid-infrared spectra were collected on a Fourier-transform infrared (FTIR) spectrometer (Spectrum Two, PerkinElmer, USA) using an attenuated total reflectance (ATR) unit with a diamond crystal. Spectra were collected from random positions within the sections within the wavenumber regions 4000–600 cm^{-1} using a resolution of 4 cm^{-1} and 10 accumulations. Each spectrum was first baseline corrected and then vector normalized by calculating the sum of the squared absorbance values of the spectrum and using the squared root of this sum as the normalization constant. For each sample group, six baseline corrected and normalized spectra were averaged.

2.7 Confocal Raman microspectroscopy

Transversal sections with a thickness of ca. 20 µm were cut with a rotary microtome (Nahita ZFP011, Auxilab, Spain). The sections were placed on glass slides in a droplet of deionized water, covered with a glass coverslip (0.17 mm thickness), and sealed with nail polish. Images were collected with a confocal Raman microscope (Renishaw InVia Qontor) equipped with a 532 nm diode laser and a Centrus 05TJ55 CCD detector behind an 830 lines/mm grating. The measurements were conducted within the spectral range between 97 and 3667 cm^{-1} using an integration time of 0.2 s and a 63× water objective (numerical aperture 1.2). Raman spectra from resin deposits within the cell lumens were acquired with 20 accumulations. Spectra from three different spots within each sample were baseline corrected, normalized to the Raman signal at ca. 974 cm^{-1}, and averaged. Raman images of latewood tracheids were measured with 220 lines per image and 220 points per line at a step size of 0.2 µm.

Confocal Raman images obtained from three different samples (untreated, resin-treated without conditioning, and resin-treated with 168 h conditioning at 33 % RH) were combined into an image mosaic. This mosaic was converted into a two-dimensional array, with the pixels as row objects and the corresponding wavenumbers in columns. Wavenumbers outside the range of 300–3600 cm^{-1} were excluded. The spectral data underwent preprocessing procedures, which included removing cosmic rays using an intensity threshold, correcting the baseline by fitting a polynomial over the selected wavenumber range, and vector normalization (Afseth et al. 2006). The intensity of the Raman band at ca. 974 cm^{-1} was quantified by integration within the range of 950–990 cm^{-1}. The resulting area values were then folded back into the image dimensions.

Furthermore, a new image mosaic was created, which included only the Raman images of the two resin-treated samples (without conditioning and 168 h conditioning at 33 % RH). This mosaic was preprocessed as described before and then mean-centered. Principal component analysis (PCA) was applied to the preprocessed, mean-centered data within the wavenumber range of 300–3600 cm^{-1} (Bro and Smilde 2014). The score values of the first principal component were used as a threshold to exclude pixels associated with strong Raman signals from water within the cell lumens. The remaining dataset was mean-centered, and the PCA was recalculated. The score values were then folded back to the image dimensions and interpreted using their corresponding loading vectors. The data analysis was conducted using a combination of custom MATLAB R2022b scripts (MathWorks, Inc.) and commercial functions from the PLS Toolbox 8.7 (Eigenvector Research, Inc.).

2.8 Statistical analysis

WPG and CWB values were tested by using one-way analysis of variance (ANOVA) to determine statistical differences between the means. Resin- and PEG-treated samples were analyzed separately, using the conditioning duration (0, 72, and 168 h) and the conditioning RH (33, 70, and 95 %) as grouping variables. Equality of variances was assumed when the p-value of Levene's test was >0.05. Multiple pairwise comparisons between sample groups were performed using the Tukey-Kramer honestly significant differences (HSD) test. All comparisons were made at a 95 % confidence level. The statistical analyses were performed using JMP Pro 16.

3 Results and discussion

3.1 Weight percent gain

All wood samples used for the analyses were cut from the same annual rings to prevent raw material-based variation from influencing the results. Thereby, a homogeneous initial dry density was achieved with little to no difference in average density between the sample groups (Table 1). With such homogeneous samples, the solid content of the treatment solution is the most important factor for the WPG in impregnation-modified wood (Altgen et al. 2020b, 2023). Therefore, the WPG measured after curing was in the narrow range between 20 and 23 % for resin- and PEG-treated samples (Table 1). ANOVA indicated no significant differences between the sample groups (separated by conditioning RH and duration) for resin-treated (p-value 0.76) and PEG-treated samples (p-value 0.96). For the resin treatment, however, there was a tendency toward slightly lower WPGs when the impregnated samples were conditioned before the heat-curing and this effect became more noticeable with increasing conditioning RH, independent of the duration. After water leaching, this trend diminished due to a stronger loss in the WPG of samples without the conditioning step. PEG-treated samples did not show such a trend.

Table 1: Average initial dry density and weight percent gain (WPG) for each sample group (n = 10).

Storage RH (%)	Storage duration (h)	Initial dry density (kg m^{-3})		WPG (%)		
		MF	PEG	MF, after curing	MF, after leaching	PEG, after curing
–	0	538 (48)	542 (46)	23.0 (3.8)	20.3 (3.3)	21.1 (3.0)
33	72	539 (45)	539 (43)	21.7 (3.1)	20.3 (3.1)	21.2 (3.2)
	168	537 (50)	538 (46)	21.7 (2.7)	20.6 (3.0)	21.3 (3.1)
70	72	537 (47)	535 (45)	21.3 (3.3)	19.8 (3.1)	21.5 (3.4)
	168	535 (43)	534 (47)	21.3 (3.2)	20.1 (3.3)	20.9 (3.3)
95	72	541 (47)	536 (47)	20.9 (3.5)	19.8 (3.5)	21.6 (3.7)
	168	539 (46)	536 (45)	20.6 (3.0)	19.8 (2.9)	20.0 (2.8)

The standard deviation is shown in parentheses.

3.2 Cell wall bulking and water vapour sorption

In contrast to the WPG, which is dependent on the uptake of chemical agents into the wood bulk irrespective of their location, the CWB only increases when chemical agents enter the wood cell walls to produce permanent swelling (Altgen et al. 2023). All treatments caused a CWB but there was a difference between resin- and PEG-treated samples (Figure 1). This difference was presumably size-related, but the actual molecular size distribution within the aqueous solutions was unknown. More importantly, the conditioning of the impregnated samples before the curing had different effects on the CWB for the MF and PEG solutions. For PEG-treated wood, the CWB was slightly higher when the samples were conditioned at 33 and 69 %, but this effect was not statistically significant (ANOVA, p-value >0.9). In contrast, there was an adverse effect of the conditioning before the drying and curing step on the CWB of resin-treated samples. Without the conditioning step, the CWB was significantly higher compared to all other sample groups (Tukey-Kramer, p-value <0.05). The CWB decreased with increasing storage duration, without a significant effect of the conditioning RH after 72 or 168 h. Water-leaching diminished the effect of storage on the CWB, but the tendency of a higher CWB without additional storage was still observed. Overall, the CWB results obtained on resin-treated samples coincided with the study by Klüppel and Mai (2013). They found lower CWB in wood treated with phenol-formaldehyde resin when the impregnated samples were stored in a desiccator over water for 1 week compared to the immediate drying and heat-curing.

The resin-treated and water-leached samples were further tested for their water sorption within the hygroscopic range (0–95 % RH) at room temperature. From the MC at the end of each RH step, the MC ratio was calculated, which related the MC of each resin-treated sample to the MC of the untreated reference sample (Figure 2). For most data points, MC ratios below 1 were calculated, which indicated an MC below the reference MC. The MC ratios decreased with rising RH during absorption and increased when the RH was lowered during desorption. While this seems to suggest a reduction in wood MC by the treatment, these trends should instead be assigned to the different sorption behaviour of the MF resin itself. The RH-dependent MC uptake of fully cured MF resin is lower compared to untreated wood (Altgen et al. 2020a). Thereby, the MC of resin-treated wood decreased because the resin in cell walls and lumens resulted only in a small increase in absorbed water mass but a large increase in the dry sample mass, which was the

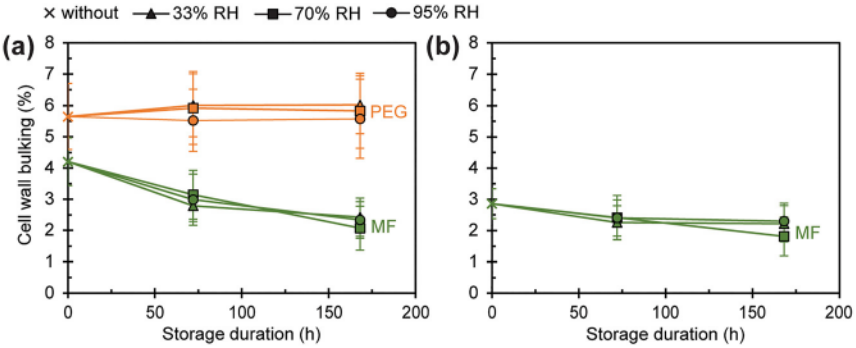

Figure 1: Cell wall bulking (CWB) of samples treated with PEG or MF resin as a function of the storage duration measured (a) after heat-curing and (b) after water-leaching (n = 10, ±standard deviation).

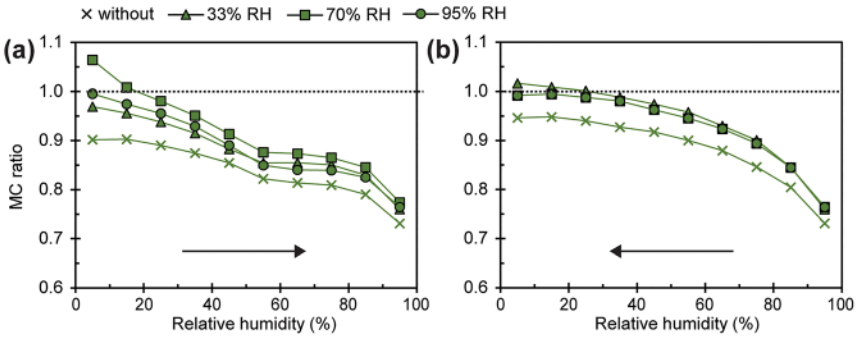

Figure 2: MC ratio ($MC_{treated}/MC_{untreated}$) as a function of the relative humidity in absorption from the dried state (a) and in desorption from the conditioned state (b). The dotted lines highlight $y = 1$ (untreated) and the arrows indicate the order of the different relative humidity steps ($n = 1$).

reference mass for the MC calculation. This effect became stronger at elevated RH as the MC difference between wood and MF resin increased, which led to the RH-dependent change in the MC ratio.

However, there were also differences in MC ratio between the sample groups despite no differences in WPG after water leaching. In particular, the MC ratio of samples without additional storage was shifted toward lower values at each RH step during ab- and desorption compared to the other resin-treated samples. A similar difference was previously observed between resin-treated samples cured under dry or non-drying (wet) conditions (Altgen et al. 2020a). A stronger reduction in the water-available cell wall space was identified as the main cause for the shift toward stronger moisture exclusion in dry-cured wood. The same effect may have applied to the present results, and this was in line with the higher CWB of samples that were immediately heat-cured without a conditioning phase.

The results showed that conditioning of impregnated samples before oven-drying and curing had either no significant effect (PEG treatment) or an adverse effect (resin treatment) on dimensional stabilization and moisture sorption. This stands in contrast to the results of Tanaka et al. (2015), who showed that conditioning solution-impregnated wood at elevated RH facilitated the diffusion of PEG into the cell walls, resulting in increased wood block dimensions even after vacuum-drying. They explained this effect by the higher solute diffusivity when more water was present in the cell wall. Several experimental details differ from the work by Tanaka et al., and one important factor may be the shorter conditioning in the present study (168 h versus 900 h). Thereby, the cell wall diffusion of PEG may have been dominated by the increase in solute concentration between the cell wall and lumen when water was removed during conditioning and/or the subsequent drying/curing (Stamm 1956).

The adverse effect of conditioning resin-treated samples, in contrast to PEG-treated samples, was in line with the presumed effect of the MF resin solution to form macromolecules that are too large to enter the cell wall, and/or to promote alkaline hydrolysis of cell wall polymers to counterbalance cell wall bulking. Both effects were tested by further analyses of the resin-treated samples.

3.3 Scanning electron microscopy

Morphological changes were observed on longitudinal-radial wood surfaces using SEM. There was no obvious difference compared to untreated wood when the impregnated samples were immediately cured (Figure 3a), but deposits of cured MF resin within the cell lumens were observed frequently in samples that were conditioned for 168 h before the curing step (Figure 3b and c). These deposits appeared in the form of small droplets on the cell walls, as reported previously (Behr et al. 2018; Mahnert et al. 2012). Previous studies on treatments with phenol-formaldehyde resin found more resin deposits in the cell lumens when there was less cell wall penetration by the resin due to higher molecule size (Biziks et al. 2020; Furuno et al. 2004;). However, MF resin deposits in cell lumens can also form a thin film covering the cell wall surfaces (Altgen et al. 2020a; Nishida et al. 2019). Since such a resin film is harder to detect by SEM, samples that were immediately cured after impregnation may have also contained resin within the cell lumens. Altgen et al. (2020b) speculated that a MF resin film covering the cell wall surfaces is formed when water is quickly removed from the cell lumens, which first results in the precipitation of the resin on the surfaces before it hardens. In contrast, the formation of droplet-shaped deposits was explained by the polycondensation of the resin in the presence of free water (Altgen et al. 2020b). Thereby, the formation of resin droplets in the conditioned samples may support the assumption that polycondensation of the resin occurred before the removal of water increased the concentration gradient to facilitate the cell wall diffusion of the resin.

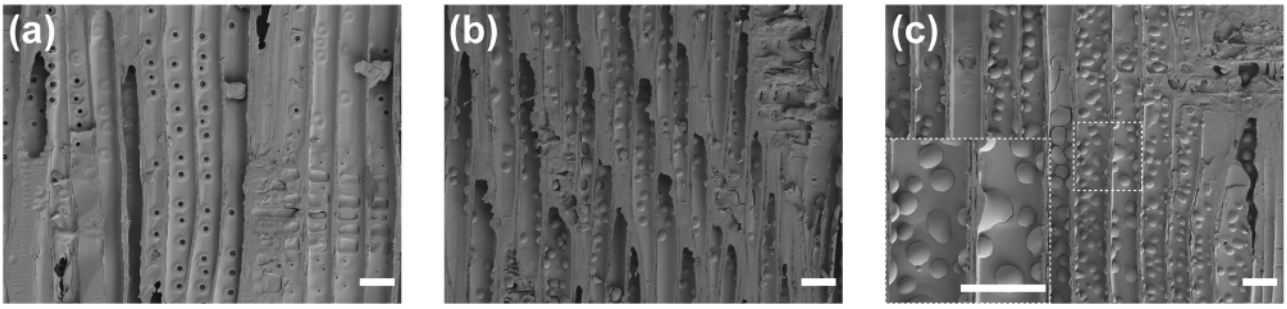

Figure 3: Scanning electron microscopy images taken from the radial surfaces of MF-treated samples that were immediately heat-cured after impregnation (a) or conditioned for 1 week at 33 % (b) or 95 % RH (c) before heat-curing (scale bars = 50 µm).

3.4 FT-IR spectroscopy

The samples were further analyzed by FTIR spectroscopy, and an assignment of important FTIR bands is listed in Supplementary Table S.1. Normalized mid-IR spectra showed a strong overlap between bands from wood and cured MF resin (Figure 4). Spectral differences between samples were particularly observed in the fingerprint region from 1800 to 600 cm^{-1}. The resin treatments resulted in an increase in absorbance at 813 and 896 cm^{-1} and within the range between 1600 and 1300 cm^{-1}, as well as in a decrease for the wood-related bands at 1733, 1232, 1102, 1051 and 1026 cm^{-1}. The latter band changes were in line with the potential alkaline hydrolysis of wood constituents. The decrease in absorbance at 1733 and 1232 cm^{-1} indicated the hydrolytic cleavage of acetyl groups in wood hemicelluloses (Pandey and Pitman 2003; Pandey and Theagarajan 1997; Zanuttini et al. 1998). The absorbance at 1102, 1051 and 1026 cm^{-1} were assigned to O–H and C–O vibrations in hemicelluloses and cellulose (Harrington et al. 1964; Pandey and Pitman 2003; Pandey and Theagarajan 1997), thus, the decrease at these bands was in line with the possible alkaline hydrolysis of amorphous wood carbohydrates. However, there were no clear differences in these bands between the different resin-treated samples.

There was little difference in the band at 813 cm^{-1} except for the general increase for the resin-treated samples compared to the untreated sample. This increase was attributed to the vibration of the triazine ring in melamine, which was observed at 810 cm^{-1} for pure MF resin and found to be insensitive to the polycondensation of the resin during heat curing (Weiss et al. 2019). The resin treatment also caused an increase in absorbance in the spectral range between 1600 and 1300 cm^{-1}. This increase was the highest for samples conditioned at 33 % RH and the lowest for samples that were immediately cured after impregnation. Presumably, these differences were not only caused by quantitative variations in the resin concentration, because this wavenumber region contains several bands that are sensitive to the curing reaction of MF resins (Merline

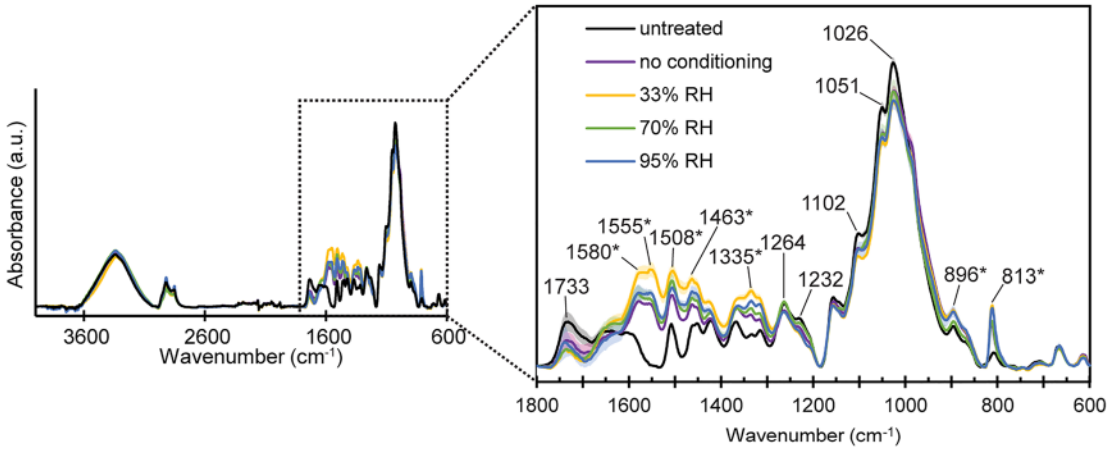

Figure 4: Baseline-corrected and vector-normalized infrared spectra of untreated and MF resin-treated wood samples in the wavenumber region 600–1800 cm^{-1}. The solid lines represent the mean (n = 6) and the shaded areas are the standard deviation of each sample group. Bands with contributions from the MF resin are marked by asterisks.

et al. 2012; Weiss et al. 2019). The transition of methylol groups in MF resin to methylene ether or methylene bridges shifts the absorption at 1355 cm^{-1} towards lower wavenumbers (Weiss et al. 2019). This band shift due to the resin cross-linking seems to have been stronger for samples that were conditioned before the curing step. MF resins contain further bands within the 1600–1300 cm^{-1} region, for example, C–NH- stretching of melamine at 1556 cm^{-1} (Kandelbauer et al. 2007), or methylene C–H bending vibrations at 1456 cm^{-1} (Merline et al. 2012). However, strong overlapping with wood-related bands made an interpretation of the spectral differences between the resin-treated samples difficult. Furthermore, the IR absorbance may have been affected by the location of the resin in the cell wall or lumens, since embedding of the resin in the cell wall structure and interaction with wood polymers potentially affected the bond vibrations.

3.5 Confocal Raman microspectroscopy

Further analyses were performed by confocal Raman microspectroscopy (Figure 5), and an assignment of important Raman bands is listed in Supplementary Table S.2. Confocal Raman microspectroscopy allowed the collection of Raman spectra from resin deposits in cell lumens without interference from Raman signals of wood (Figure 5a). The resin spectra were normalized to the intense band at 974 cm^{-1}, which was assigned to the triazine-ring nitrogen radial in-phase vibration of melamine (Larkin et al. 1999). This band has been shown to remain unaffected by the curing of MF resin (Scheepers et al. 1993, 1995). All obtained spectra showed the typical features of cured MF resin, as reported previously (Altgen et al. 2020b). Nonetheless, spectral variations indicating differences in the cross-linked resin structure between the treated samples were observed. The biggest differences in the resin spectra were observed between the sample that was conditioned at 33 % and the resin-treated samples without the conditioning step. The resin spectrum obtained from the non-conditioned samples had a lower Raman signal within the region from 550 to 800 cm^{-1} that contains in-plane (677 cm^{-1}) and out-of-plane bending vibrations of the triazine ring (745 cm^{-1}) that are sensitive to the resin cross-linking (Altgen et al. 2020a; Scheepers et al. 1993). This sample also showed a lower signal at 1559 cm^{-1}, which may be attributed to C–H bending (Larkin et al. 1999). In contrast, the sample that was conditioned at 33 % RH showed stronger band changes that are typically associated with the cleavage of methyl ether groups in the partially methylated MF resin or the transformation of ether linkages to methylene bridges by elimination of formaldehyde. This was observed by the lower Raman signal for the band at 907 cm^{-1} and for the shoulder at around 1000 cm^{-1}, as well as the stronger broadening of the band at 1448 cm^{-1} (methylol groups) toward smaller wavenumbers.

Conditioning the resin-impregnated samples for several days may have affected the MF resin cure. Although the cross-linking reactions of MF resins progress slowly at room temperature, they are catalyzed by mixing with acidic wood (Bergmann et al. 2006). The conditioning may have promoted the cleavage of methyl ether groups in the partially methylated resin, which would have increased the amount of methylol groups available for cross-linking during the subsequent curing step. Furthermore, some methylene bridges may have been formed already during the conditioning phase before the actual curing step. However, the Raman spectra of the resin deposits also showed variation between the conditioned samples. This variation did not follow any clear trend that could be related to the conditioning RH; hence, there remains uncertainty about the exact effects of the conditioning step on the MF resin cure.

Since the biggest differences in the FTIR and Raman spectra were observed between samples conditioned at 33 % and samples that were immediately cured without conditioning, these two samples were selected for confocal Raman mapping of latewood cell walls at sub-micron resolution. Average spectra collected from the secondary cell walls showed an increased signal at 631, 974, 1330 and 1451 cm^{-1} compared to the Raman spectrum of untreated wood (Figure 5b), which coincided with Raman bands found in pure MF resin. The spatial distribution of the MF resin was visualized by band integration in the spectral region from 950 to 990 cm^{-1} in each pixel of the Raman images (Figure 5c). Untreated cell walls only had a small Raman signal in this spectral region, and this was increased in the treated samples due to the presence of MF resin. The effect of the resin treatment was also visible as a shift of the main peak in the pixel histograms toward higher band areas (Figure 5d). The increase in Raman signal at 974 cm^{-1} within the cell walls was slightly higher when the treatment was done without the conditioning step. This increase in Raman signal was evident across the entire cell walls (Figure 5c). The Raman signal of the cell walls was slightly lower when a conditioning step was done before the curing, but the cell wall regions near the lumens showed high Raman signals. While this indicated a hindered diffusion of MF resin through the cell walls, it may have also been related to potential within-sample variation, which is difficult to consider with Raman mapping at sub-micron resolution. In any case, the Raman images based on the signal at 974 cm^{-1} did not show an improvement in the resin uptake of the cell wall caused by a 1 week conditioning step, in line with the CWB results.

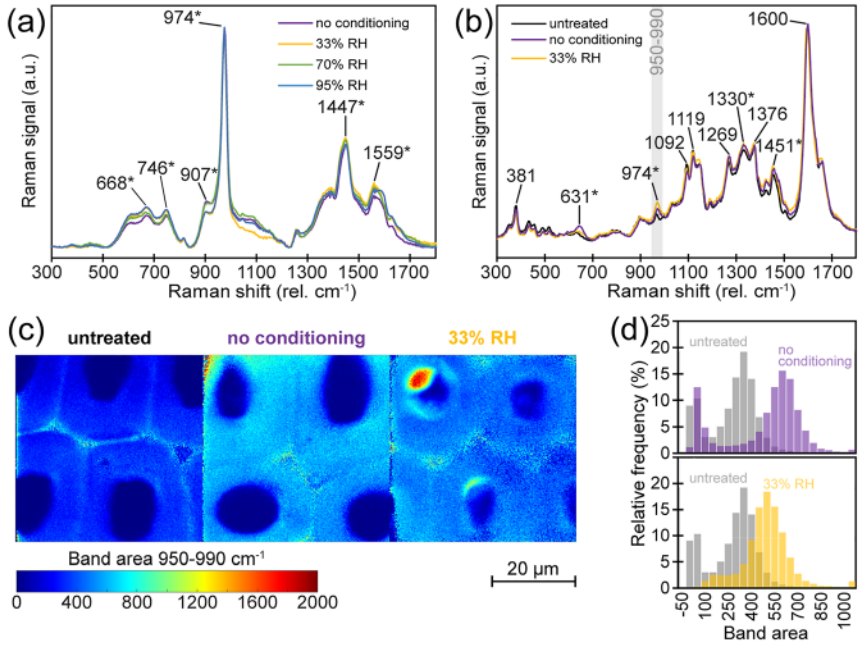

Figure 5: Results of confocal Raman microspectroscopy on thin wood sections from untreated and MF resin-treated wood samples: average Raman spectra of resin deposits in cell lumen normalized to the signal at 974 cm^{-1} (a); average Raman spectra of secondary cell walls (b); Raman images based on band integration at 950–990 cm^{-1} (c); and corresponding pixel histograms (d). Bands with contributions from the MF resin are marked by asterisks.

Further variation in the Raman spectra between the two resin-treated samples was investigated by PCA which considered the entire spectral range. After removing pixels associated with water within the cell lumens, the first five principal components (PCs) explained ca. 64 % of the variation within the image mosaic. The first three PCs explained within-sample variation, which was related to residual pixels near the lumen with large spectral contributions from water, or to the natural variation in lignin and carbohydrate contents between compound middle lamella and the secondary cell wall (Supplementary Figure S.1). However, PCs four and five also showed an inter-sample variation that could be due to different treatment conditions (Figure 6).

The loadings of PC four (Figure 6a) contained positive bands that were assigned to MF resin (647 and 974 cm^{-1}) (Altgen et al. 2020b; Scheepers et al. 1993) and to lignin (1607 cm^{-1}) (Agarwal and Ralph 1997). The loadings also showed a positive band at 2955 cm^{-1} and a negative band at 2882 cm^{-1}. Presumably, this separated the broad CH/CH_2 stretching band from wood at 2800–3000 cm^{-1} based on the contributions from lignin at higher wavenumbers (2845–3075 cm^{-1}) and wood carbohydrates at lower wavenumbers (2820–2970 cm^{-1}) (Agarwal and Ralph 1997; Agarwal et al. 2011; Blackwell et al. 1970; Edwards et al. 1994). In line with these assignments, the corresponding score image showed high scores in the lignin-rich middle lamella and cell corners and some resin-rich regions of the cell walls near the lumen. In contrast, the loadings of PC five (Figure 6b) showed a positive lignin band at ca. 1604 cm^{-1} and negative bands at 970, 1444, and 1552 cm^{-1}, which were assigned to the MF resin. Thereby, the corresponding score image showed positive scores in the lignin-rich regions and negative scores in cell wall regions with high resin content.

PCs four and five showed variation between the two resin-treated samples based on the scores of the secondary cell walls. For both PCs, lower scores were observed within

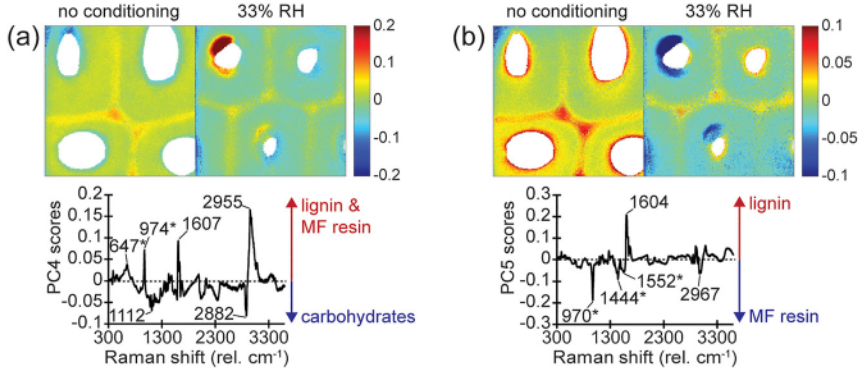

Figure 6: Results of the principal component analysis (PCA) applied to an image mosaic based on confocal Raman mapping of MF resin-treated wood samples that were either cured immediately after impregnation or after conditioning at 33 % RH for 168 h. Score images with corresponding loading vectors are shown for principal components four (a) and five (b). Bands with contributions from the MF resin are marked by asterisks.

the cell walls of the conditioned sample. This is presumably unrelated to differences in resin content because the triazine ring vibration in the MF resin near 974 cm^{-1} was positive in the loading vector of PC four and negative for PC five. However, in PC four, the triazine ring vibration at 974 cm^{-1} was accompanied by a band at 647 cm^{-1}, which belonged to the broad band structure in MF resin at 550–800 cm^{-1}. In PC five, the triazine ring vibration shifted to 970 cm^{-1} and was accompanied by bands at 1444 and 1552 cm^{-1}, which belonged to the MF resin band structure in the 1300–1700 cm^{-1} region. Although it is difficult to link these differences to specific curing reactions, the results indicated that the conditioning step may have not only affected the resin cure within the cell lumen but also in the wood cell wall.

4 Conclusions

Applying a conditioning step at room temperature to impregnated wood samples had an adverse effect on the dimensional stabilisation achieved with a melamine formaldehyde resin, irrespective of the conditioning RH. The results supported the hypothesis that this adverse effect was related to the alkaline hydrolysis of wood components and the resin polycondensation in the cell lumens during the conditioning step. However, the present study did not consider the treatment of larger wood dimensions, during which the translocation of the resin solution through the capillary network of wood becomes important. Future studies may determine if a conditioning step helps in controlling this resin translocation.

Acknowledgments: This work made use of the Aalto University Nanomicroscopy Center (AaltoNMC) premises.

Research ethics: Not applicable.

Author contributions: T.S. and M.A. designed the experiments and conducted the water sorption and confocal Raman microspectroscopy measurements. T.S. performed the wood treatments and recorded the infrared spectra. M. Aw. applied PCA to the confocal Raman data. D.A. performed the SEM analyses. M.A. analysed the results together with T.S. and wrote the manuscript, which was reviewed by all authors.

Competing interests: The authors state no conflicts of interest.

Research funding: This work received funding from the Research Council of Finland (grant no. 341701).

Data availability: The raw data can be obtained on request from the corresponding author.

References

Afseth, N.K., Segtnan, V.H., and Wold, J.P. (2006). Raman spectra of biological samples: a study of preprocessing methods. Appl. Spectrosc. 60: 1358–1367.

Agarwal, U.P. and Ralph, S.A. (1997). FT-Raman spectroscopy of wood: identifying contributions of lignin and carbohydrate polymers in the spectrum of black spruce (*Picea mariana*). Appl. Spectrosc. 51: 1648–1655.

Agarwal, U.P., McSweeny, J., and Ralph, S.A. (2011). FT-Raman investigation of milled-wood lignins: softwood, hardwood, and chemically modified black spruce lignins. J. Wood Chem. Technol. 31: 324–344.

Altgen, M., Altgen, D., Klüppel, A., and Rautkari, L. (2020a). Effect of curing conditions on the water vapor sorption behavior of melamine formaldehyde resin and resin-modified wood. J. Mater. Sci. 55: 11253–11266.

Altgen, M., Awais, M., Altgen, D., Klüppel, A., Mäkelä, M., and Rautkari, L. (2020b). Distribution and curing reactions of melamine formaldehyde resin in cells of impregnation-modified wood. Sci. Rep. b10: 3366.

Altgen, M., Awais, M., Altgen, D., Klüppel, A., Koch, G., Mäkelä, M., Olbrich, A., and Rautkari, L. (2023). Chemical imaging to reveal the resin distribution in impregnation-treated wood at different spatial scales. Mater. Des. 225: 111481.

Behr, G., Bollmus, S., Gellerich, A., and Militz, H. (2018). The influence of curing conditions on the properties of European beech (*Fagus sylvatica*) modified with melamine resin assessed by light microscopy and SEM-EDX. Int. Wood Prod. J. 9: 22–27.

Bergmann, I., Müller, U., Rätzsch, M., and Steiner, M. (2006). Investigations on the crosslinking reactions of melamine resins in the presence of wood. Monatshefte für Chem. Chem. Mon. 137: 881–886.

Biziks, V., Bicke, S., Koch, G., and Militz, H. (2020). Effect of phenol-formaldehyde (PF) resin oligomer size on the decay resistance of beech wood. Holzforschung 75: 574–583.

Blackwell, J., Vasko, P.D., and Koenig, J.L. (1970). Infrared and Raman spectra of the cellulose from the cell wall of *Valonia ventricosa*. J. Appl. Phys. 41: 4375–4379.

Bro, R. and Smilde, A.K. (2014). Principal component analysis. Anal. Methods 6: 2812–2831.

Edwards, H.G.M., Farwell, D.W., and Williams, A.C. (1994). FT-Raman spectrum of cotton: a polymeric biomolecular analysis. Spectrochim. Acta Part Mol. Spectrosc. 50: 807–811.

Furuno, T., Imamura, Y., and Kajita, H. (2004). The modification of wood by treatment with low molecular weight phenol-formaldehyde resin: a properties enhancement with neutralized phenolic-resin and resin penetration into wood cell walls. Wood Sci. Technol. 37: 349–361.

Greenspan, L. (1977). Humidity fixed points of binary saturated aqueous solutions. J. Res. Natl. Bur. Stand. - Phys. Chem. 81 A: 89–96.

Harrington, K.J., Higgins, H.G., and Michell, A.J. (1964). Infrared spectra of *Eucalyptus regnans* F. Muell. and *Pinus radiata* D. Don. Holzforschung 18: 108–113.

Hu, J., Fu, Z., Wang, X., and Chai, Y. (2022). Manufacturing and characterization of modified wood with in situ polymerization and cross-linking of water-soluble monomers on wood cell walls. Polymers 14: 3299.

Jakes, J.E., Hunt, C.G., Zelinka, S.L., Ciesielski, P.N., and Plaza, N.Z. (2019). Effects of moisture on diffusion in unmodified wood cell walls: a phenomenological polymer science approach. Forests 10: 1084.

Jeremic, D., Cooper, P., and Heyd, D. (2007). PEG bulking of wood cell walls as affected by moisture content and nature of solvent. Wood Sci. Technol. 41: 597–606.

Kandelbauer, A., Despres, A., Pizzi, A., and Taudes, I. (2007). Testing by Fourier transform infrared species variation during melamine–urea–formaldehyde resin preparation. J. Appl. Polym. Sci. 106: 2192–2197.

Klüppel, A. and Mai, C. (2013). The influence of curing conditions on the chemical distribution in wood modified with thermosetting resins. Wood Sci. Technol. 47: 643–658.

Larkin, P.J., Makowski, M.P., and Colthup, N.B. (1999). The form of the normal modes of s-triazine: infrared and Raman spectral analysis and ab initio force field calculations. Spectrochim. Acta. A. Mol. Biomol. Spectrosc. 55: 1011–1020.

Mahnert, K.-C., Adamopoulos, S., Koch, G., and Militz, H. (2012). Topochemistry of heat-treated and N-methylol melamine-modified wood of koto (*Pterygota macrocarpa* K. Schum.) and limba (*Terminalia superba* Engl. et Diels). Holzforschung 67: 137–146.

Merline, D.J., Vukusic, S., and Abdala, A.A. (2012). Melamine formaldehyde: curing studies and reaction mechanism. Polym. J. 45: 413–419.

Nishida, M., Tanaka, T., Miki, T., Hayakawa, Y., and Kanayama, K. (2019). Integrated analysis of modified Japanese cypress using solid-state NMR spectra and nuclear magnetic relaxation times. Cellulose 26: 3625–3642.

Ohmae, K., Minato, K., and Norimoto, M. (2002). The analysis of dimensional changes due to chemical treatments and water soaking for hinoki (Chamaecyparis obtusa) wood. Holzforschung 56: 98–102.

Pandey, K.K. and Pitman, A.J. (2003). FTIR studies of the changes in wood chemistry following decay by brown-rot and white-rot fungi. Int. Biodeterior. Biodegrad. 52: 151–160.

Pandey, K.K. and Theagarajan, K.S. (1997). Analysis of wood surfaces and ground wood by diffuse reflectance (DRIFT) and photoacoustic (PAS) Fourier transform infrared spectroscopic techniques. Holz Als Roh-Werkst 55: 383–390.

Scheepers, M.L., Gelan, J.M., Carleer, R.A., Adriaensens, P.J., Vanderzande, D.J., Kip, B.J., and Brandts, P.M. (1993). Investigation of melamine-formaldehyde cure by Fourier transform Raman spectroscopy. Vib. Spectrosc. 6: 55–69.

Scheepers, M.L., Meier, R.J., Markwort, L., Gelan, J.M., Vanderzande, D.J., and Kip, B.J. (1995). Determination of free melamine content in melamine-formaldehyde resins by Raman spectroscopy. Vib. Spectrosc. 9: 139–146.

Stamm, A.J. (1934). Effect of inorganic salts upon the swelling and the shrinking of wood. J. Am. Chem. Soc. 56: 1195–1204.

Stamm, A.J. (1956). Dimensional stabilization of wood with carbowaxes. For. Prod. J. 6: 201–204.

Tanaka, S., Seki, M., Miki, T., Shigematsu, I., and Kanayama, K. (2015). Solute diffusion into cell walls in solution-impregnated wood under conditioning process I: effect of relative humidity on solute diffusivity. J. Wood Sci. 61: 543–551.

Thybring, E.E. (2013). The decay resistance of modified wood influenced by moisture exclusion and swelling reduction. Int. Biodeterior. Biodegrad. 82: 87–95.

Thygesen, L.G., Ehmke, G., Barsberg, S., and Pilgård, A. (2020). Furfurylation result of Radiata pine depends on the solvent. Wood Sci. Technol. 54: 929–942.

Weiss, S., Urdl, K., Mayer, H.A., Zikulnig-Rusch, E.M., and Kandelbauer, A. (2019). IR spectroscopy: suitable method for determination of curing degree and crosslinking type in melamine–formaldehyde resins. J. Appl. Polym. Sci. 136: 47691.

Zanuttini, M., Citroni, M., and Martínez, M.J. (1998). Application of diffuse reflectance infrared Fourier transform spectroscopy to the quantitative determination of acetyl groups in wood. Holzforschung 52: 263–267.

Zheng, P., Aoki, D., Seki, M., Miki, T., Tanaka, S., Kanayama, K., Matsushita, Y., and Fukushima, K. (2018). Visualization of solute diffusion into cell walls in solution-impregnated wood under varying relative humidity using time-of-flight secondary ion mass spectrometry. Sci. Rep. 8: 9819.

Supplementary Material: This article contains supplementary material (https://doi.org/10.1515/hf-2023-0084).